Ti(IV), Cr(III), Mn(II), and Ni(II) Complexes of the Norfloxacin Antibiotic Drug: Spectroscopic and Thermal Characterizations

Moamen S. Refat*,†,‡ and Gehad G. Mohamed§

Department of Chemistry, Faculty of Science, Suez Canal University, Port Said 42111, Egypt, Department of Chemistry, Faculty of Science, Taif University, 888 Taif, Kingdom of Saudi Arabia, and Chemistry Department, Faculty of Science, Cairo University, Egypt

Eleven new complexes of norfloxacin (HL) with the formulas $[Ti(HL)(Cl)_4]$, $[Cr_2(L)_2(CO_3)_2(H_2O)_4]$, $[Cr(HL)_2(Cl)_2]Cl\cdot 3H_2O$, $[Cr(HL)_2(AcO)_2]AcO\cdot 2H_2O$, $[Cr_2(HL)_2(SO_4)_2(H_2O)_4]SO_4$, $[Mn(L)_2(H_2O)_2]$, $[Mn(HL)_2(Cl)_2]$, $[Mn(HL)_2(AcO)_2]$, $[Ni(HL)_2(Cl)_2]$, $[Ni(HL)_2(SO_4)]$, and $[Ni(HL)_2(AcO)_2]$ have been synthesized and studied using spectroscopic and thermal analysis techniques. The thermal decomposition processes of these complexes are discussed. The activation energies, E^*, the pre-exponential factor, A, the entropies, ΔS^*, enthalpies, ΔH^*, and Gibbs energies, ΔG^*, of the thermal decomposition reactions have been derived from thermogravimetric (TG) and differential thermogravimetric (DTG) curves. Using the Coats−Redfern and Horowitz−Metzeger methods, kinetic analysis of the thermogravimetric data is performed.

Introduction

The term quinolones is commonly used for the quinolonecarboxylic acids or 4-quinolones, which are a group of synthetic antibacterial agents containing a 4-oxo-1,4-dihydroquinoline skeleton. Since the introduction of nalidixic acid[1] into clinical practice in the early 1960s, a number of structurally related highly potent broad-spectrum antibacterial agents have been isolated.[1,2]

Modifications to nalidixic acid have been made based on structure activity relationships. It was discovered that a fluorine atom at position 6 and a piperazine ring at position 7 greatly enhance the spectrum of activity. The fluoroquinolones are very active against aerobic Gram-negative microorganisms but less active against Gram-positive microorganisms.[1,3] They are extremely useful for the treatment of a variety of infections, including urinary tract infections, soft tissue infections, respiratory infections, bone-joint infections, typhoid fever, sexually transmitted diseases, prostatitis, community acquired pneumonia, acute bronchitis, and sinusitis.[1,2,4] Recently, a relatively new approach to the rational design of antitumor agents has been introduced using some new quinolone molecules that display a novel mode of action.[5]

Fluoroquinolones belong to a group of synthetic antibiotics that are derived from the basic structure of nalidixic acid and have substituents at N-1, C-5, C-7, and position 8 and a fluorine atom at position 6. There are also polycyclic derivatives. Quinolone antibiotics have a ketone at position 4 and a carboxylic group at position 3. Fluoroquinolones inhibit the bacterial DNA gyrase or the topoisomerase IV enzyme, resulting in the inhibition of DNA replication and transcription. Fluorine at position 6 enhances gyrase inhibition and cell penetration. Piperazinyl substituents provide activity against Gram-negative bacteria, and the pyrrolidinyl moiety is active against Gram-positive cocci. They improve water solubility needed oral application. The function substituted at position 8 is to control anaerobe activity. The uptake of norfloxacin (Figure 1) by *Escherichia coli* has been investigated at different pH and monovalent/divalent metal ion concentrations.[6] The results of the study supported a simple diffusion mechanism for quinolone incorporation into cells. The uptake process decreases under acidic conditions. The presence of Na^+ and K^+ ions does not affect the results to an appreciable extent, whereas divalent ions cause a dramatic decrease in drug incorporation. The antibacterial activity evaluated under identical experimental conditions shows a direct relationship with the uptake data. It was suggested that the ability of the drug to penetrate into cells is a function of its net charge. The molecule in zwitterionic form exhibits maximum permeation properties, whereas the uptake is strongly reduced when the drug bears a net charge as a result of ionization or complex formation with divalent ions.

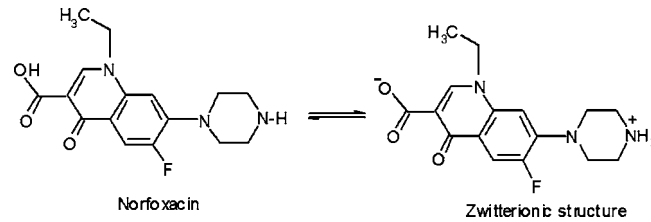

Figure 1. Structure of norfloxacin and its zwitterionic form.

The proposed mechanism of the interaction between quinolone and metal cations was chelation between the metal and the 4-oxo and adjacent carboxyl groups. Since these functional groups are required for antibacterial activity, it could be anticipated that all of the quinolones will interact with metal ions. However, there may be differences between the quinolones regarding the extent of interaction.[7] The crystal structures of several free quinolone molecules have been determined: nalidixic acid,[8,9] pefloxacin methanesulfonate,[10,11] cinoxacin,[12] norfloxacin (nfH),[13,14] ciprofloxacin hexahydrate,[15] ciprofloxacin lactate,[16] and norfloxacin dihydrochloride.[17,18]

It is interesting to note that in most cases the carboxylic group is not deprotonated and the hydrogen atom of this group is

* Corresponding author. E-mail address: msrefat@yahoo.com.
† Suez Canal University.
‡ Taif University.
§ Cairo University.

10.1021/je100064h
Published on Web 06/07/2010

Table 1. Elemental Analysis, Molar Conductance, and Magnetic Measurement Data of the Norfloxacin Complexes

	(calcd) found				molar conductance	
complexes (formula/M_w)	%C	%H	%N	%M	$\Omega^{-1}\cdot cm^2\cdot mol^{-1}$	μ_{eff}
$[Ti(HL)Cl_4]$/509.23	(37.70)	(3.53)	(8.24)	(9.41)	46	1.71
	37.12	3.33	8.14	9.34		
$[Cr_2(L)_2(CO_3)_2(H_2O)_4]$/932.65	(43.74)	(4.50)	(9.00)	(11.15)	10	3.77
	43.22	4.37	8.56	11.09		
$[Cr(HL)_2Cl_2]Cl\cdot 3H_2O$/851.16	(45.11)	(4.93)	(9.87)	(6.11)	76	3.90
	44.97	4.87	9.76	5.97		
$[Cr(HL)_2(AcO)_2]AcO\cdot 2H_2O$/903.66	(50.46)	(5.42)	(9.29)	(5.75)	19	3.75
	50.36	5.23	9.11	5.49		
$[Cr_2(HL)_2(SO_4)_2(H_2O)_4]SO_4$/1102.65	(34.82)	(3.99)	(7.62)	(9.43)	19	3.86
	34.68	3.59	7.49	9.29		
$[Mn(L)_2(H_2O)_2]$/727.60	(52.78)	(5.22)	(11.54)	(7.55)	12	5.90
	52.66	5.17	11.44	7.37		
$[Mn(HL)_2Cl_2]$/764.60	(50.22)	(4.71)	(10.99)	(7.18)	32	5.96
	50.02	4.59	10.85	7.04		
$[Mn(HL)_2(AcO)_2]$/811.60	(53.23)	(5.17)	(10.35)	(6.77)	15	5.88
	53.10	4.97	10.29	6.68		
$[Ni(HL)_2Cl_2]$/768.36	(49.98)	(4.68)	(10.93)	(7.64)	36	3.50
	49.59	4.60	10.84	7.55		
$[Ni(HL)_2SO_4]$/793.36	(48.40)	(4.54)	(10.59)	(7.40)	22	3.83
	48.16	4.43	10.48	7.22		
$[Ni(HL)_2(AcO)_2]$/815.36	(52.98)	(5.15)	(10.30)	(7.20)	15	3.85
	52.76	5.04	10.21	7.05		

Table 2. Main IR Peaks of Norfloxacin and Its Complexes[a]

compound	ν(C═O)	ν(COO)(asym)	ν(COO)(sym.)	ν(C═O)(carbonyl)	ν(M—O)
norfloxacin	1727sh	1590sh	1396sh	1716sh	
$[Ti(HL)Cl_4]$	1712sh	1594s	1395m	1629sh	520s
					499s
					473s
$[Cr_2(L)_2(CO_3)_2(H_2O)_4]$	1731sh	1550w	1374m	1616sh	515w
					499w
					466w
$[Cr(HL)_2Cl_2]Cl\cdot 3H_2O$	1721sh	1594w	1379m	1691sh	523w
					495s
					475w
$[Cr(HL)_2(AcO)_2]AcO\cdot 2H_2O$	1709w	1584s	1382m	1689w	522w
					499w
					460w
$[Cr_2(HL)_2(SO_4)_2(H_2O)_4]SO_4$	dis.	1552s	1383m	1631sh	522s
					500s
					420w
$[Mn(L)_2(H_2O)_2]$	dis.	1581m	1383sh	1628sh	527s
					499s
					478w
$[Mn(HL)_2Cl_2]$	1691w	1573m	1384s	1627sh	527s
					506s
					476w
$[Mn(HL)_2(AcO)_2]$	dis.	1580sh	1376sh	1615sh	525w
					507s
					474s
$[Ni(HL)_2Cl_2]$	dis.	1574sh	1383m	1630sh	525s
					510s
					476s
$[Ni(HL)_2SO_4]$	dis.	1572sh	1385sh	1630sh	523s
					508s
					460s
$[Ni(HL)_2(AcO)_2]$	dis.	1574sh	1394sh	1631sh	529s
					499s
					464s

[a] sh = sharp, m = medium, s = small, w = weak.

hydrogen-bonded to an adjacent 4-oxo atom. In a few examples,[13−15] the carboxylic group is ionized, and the molecule thus exists in a zwitterionic form with a protonated terminal nitrogen of the piperazine ring in a solid state. A complex of magnesium(II) with the formula $[Mg_2(H_2O)_6(nfH)_2]Cl_4$ was isolated by a hydrothermal reaction.[19] It can be described as a 2:2 dimer in which the two magnesium ions are bridged by two oxygen atoms from carboxylate groups of the two norfloxacin molecules.

The coordination mode of carboxylate can be considered as a monodentate bridging type. A calcium complex, $[Ca_2(Cl)(nfH)_6]Cl_3$, was also isolated by a hydrothermal reaction.[19] This complex is also a dimer, but the bridging group is a chloride ion. The coordination geometry around each calcium ion can best be described as a distorted pentagonal bipyramid.

Four chloride ions are coordinated to a copper(II) ion, in forming the rather distorted tetrahedron in (nfH3)(nfH2)$[CuCl_4]Cl$.[18] There are two nonequivalent norfloxacin molecules

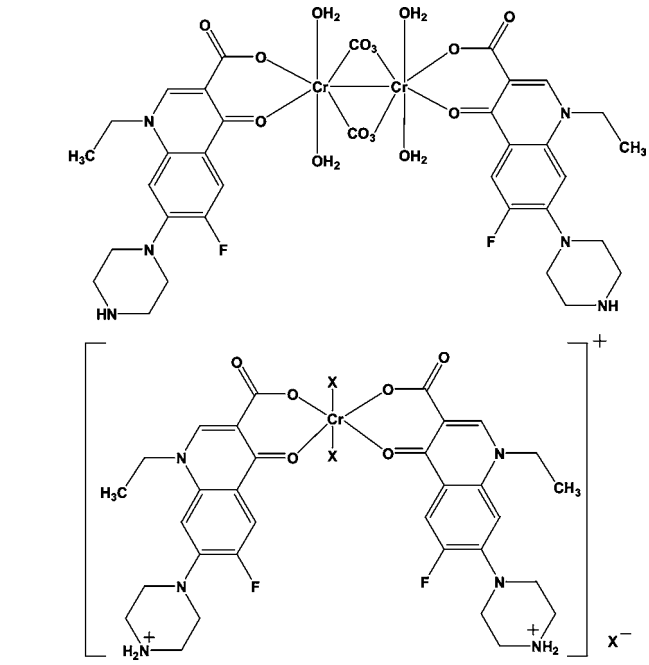

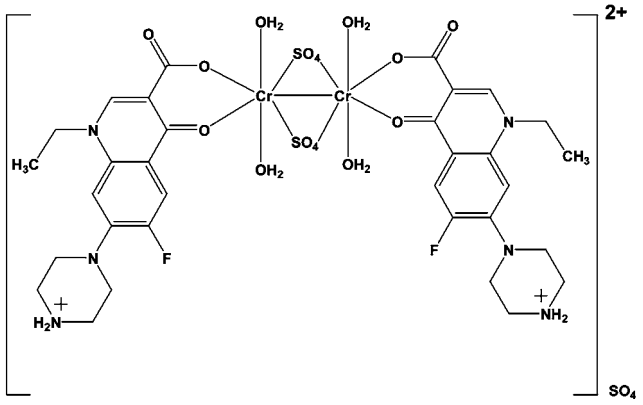

Figure 2. Structures of Cr(III) norfloxacin complexes.

in the asymmetric unit. Also, the zinc compound (nfH3)-(nfH2)[$ZnCl_4$]Cl[18] is isotypical to the copper/norfloxacin compound.

According to our previous work,[20−22] dealing with the synthesis and characterization of new metal complexes with quinolone, these antibacterial agents have great importance for understanding drug−metal ion interaction that takes into account their potential pharmacological use. The objective of this study is the isolation and characterization of the Ti(IV), Cr(III), Mn(II), and Ni(II) norfloxacin complexes, as well as their characterization using spectroscopic and thermal analysis techniques. The thermal behavior of these complexes was studied. The antibacterial activity of the investigated complexes was tested against *E. coli* (Gram − ve) and *Bacillus subtilis* (Gram + ve), and antifungal activity was also investigated (tricoderma and penicillium activities).

Experimental Section

Materials. Norfloxacin was received from the Egyptian International Pharmaceutical Industrial Company (EIPICO). All chemicals used for the preparation of the complexes were of analytical reagent grade, commercially available, used without further purification, and received from different sources (Fluka and Aldrich).

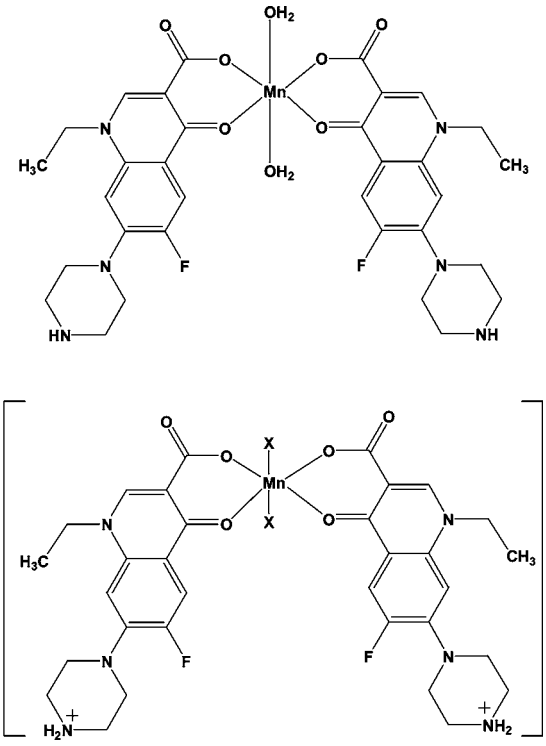

Figure 3. Structures of Mn(II) norfloxacin complexes.

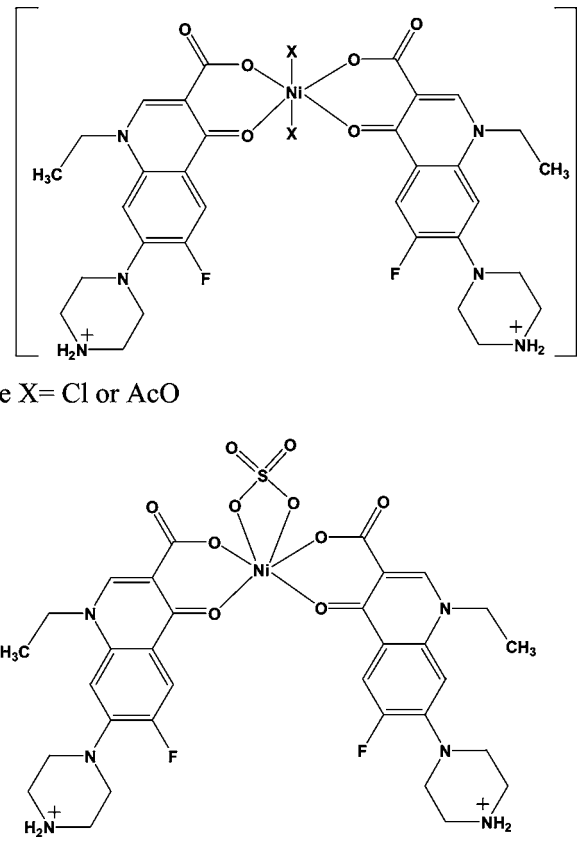

Figure 4. Structures of Ni(II) norfloxacin complexes.

Synthesis of Norfloxacin Metal Complexes. All of the norfloxacin complexes were prepared as follows, employing a 1:2 (metal ions/HL) ratio (except for the titanium(IV) complex where a 1:4 ratio was used). A solution of 1.0 mmol of each salt of Ti(IV), Cr(III), Mn(II), and Ni(II) previously dissolved

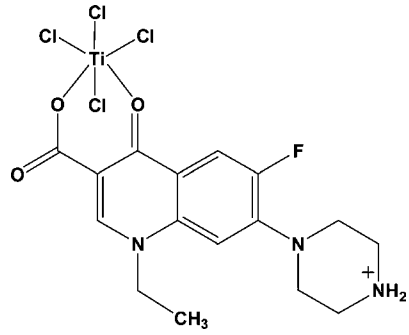

Figure 5. Structures of Ti(IV) norfloxacin complex.

in 5 mL of distilled water was added to a suspended solution of (2.0 or 4.0) mmol of norfloxacin in 50 mL of acetone. The resulting mixtures were heated at ~75 °C under reflux on a water bath for about 24 h and then cooled. The obtained complexes were separated from the reaction mixture by filtration, washed with boiling water and acetone, and dried under vacuum over $CaCl_2$.

Instrumental. CHN contents were determined using a Perkin-Elmer CHN 2400. The Ti(IV), Cr(III), Mn(II), and Ni(II) percentages were estimated gravimetrically by the direct ignition of these complexes at 800 °C for 3 h until constant weight. The residuals were then weighed in the form of metal oxides. IR spectra were recorded on a Bruker Fourier transform infrared (FTIR) spectrophotometer [(4000 to 400) cm^{-1}] in KBr pellets. The UV−vis spectra were performed in a DMSO solvent with concentration ($1.0 \cdot 10^{-3}$ M) for both the free norfloxacin ligand and its complexes using a Jenway 6405 spectrophotometer with 1 cm quartz cells in the range of (800 to 200) nm. The solid reflectance spectra were performed on a Shimadzu 3101pc spectrophotometer. Magnetic measurements were carried out on a Sherwood Scientific magnetic balance using the Gouy method with $Hg[Co(CNS)_4]$ and $[Ni(en)_3](S_2O_3)$ as calibrants. Molar conductivities of the freshly prepared solutions with a concentration of $1.0 \cdot 10^{-3}$ mol·L^{-1} in dimethylsulfoxide (DMSO) were measured using a Jenway 4010 conductivity meter. Thermogravimetric analyses (TG/DTG and DTA) were carried out in a dynamic nitrogen atmosphere (30 mL·min^{-1}) with a heating rate of 10 °C·min^{-1} using a Schimadzu TGA-50H thermal analyzer.

Anion analysis was performed as follows: the complexes were dissolved in 5 mL concentrated HNO_3 and the obtained samples diluted with water to 25 mL. The qualitative analysis of the Cl^- and SO_4^{2-} ions were performed by reactions with $AgNO_3$ and $BaCl_2$ solutions, respectively.

Antibacterial Investigation. The procedure described by Gupta et al.[23] was employed. The investigated isolates of bacteria were seeded in tubes with nutrient broth (NB). The seeded NB (1 mL) was homogenized in the tubes with 9 mL of melted (45 °C) nutrient agar (NA). The homogeneous suspensions were poured into Petri dishes and left until solidified. Some holes were spread on the top of the solidified media. Holes having a diameter of 4 mm were impregnated with $2 \cdot 10^{-3}$ dm^3 of the test. After incubation for 24 h in a thermostat at 25 °C, the inhibition (sterile) zone diameters (including disk) were measured and expressed in millimeters. An inhibition zone diameter over 7 mm indicates that the tested compound is active against the bacteria under investigation.

The antibacterial activities of the investigated compounds were tested against *Escherichia coli* (Gram − ve) and *Bacillus subtilis* (Gram + ve), as well as for antifungal activity (tricoderma and penicillium).

Results and Discussion

The analytical data show the formula of norfloxacin complexes as: $[Ti(HL)Cl_4]$ (yellowish white), $[Cr_2(L)_2(CO_3)_2(H_2O)_4]$ (green), $[Cr(HL)_2Cl_2]Cl \cdot 3H_2O$ (dark green), $[Cr(HL)_2(AcO)_2]$-$AcO \cdot 2H_2O$ (bluish green), $[Cr_2(HL)_2(SO_4)_2(H_2O)_4]SO_4$ (green), $[Mn(L)_2(H_2O)_2]$ (buff), $[Mn(HL)_2Cl_2]$ (buff), $[Mn(HL)_2(AcO)_2]$ (pink), $[Ni(HL)_2Cl_2]$ (light green), $[Ni(HL)_2SO_4]$ (light green), and $[Ni(HL)_2(AcO)_2]$ (green). The test for anions is positive only after decomposing the complexes with concentrated HNO_3, indicating most of them are bound inside the coordination sphere. All norfloxacin complexes are solids, colored, and freely soluble in dimethylformamide (DMF) or DMSO. Conductivity measurements in dimethylsulfoxide indicated them to be slightly conductive [(10 to 76) $\Omega^{-1} \cdot cm^2 \cdot mol^{-1}$)].[21,22] All compounds gave satisfactory elemental analysis results as shown in Table 1. All complexes were decomposed over 250 °C indicating their thermal stability.

Infrared Spectra. The IR data of norfloxacin and its Ti(IV), Cr(III), Mn(II), and Ni(II) complexes are listed in Table 2. The IR spectra of the complexes are compared with those of the free ligand to determine the coordination sites that may involved in chelation. There are some guide peaks, in the spectra of the ligand, which are useful in achieving this goal. The position and/or the intensities of these peaks are expected to be changed upon chelation. These guide peaks are listed in Table 2. The ν(OH), ν(C═O), ν_{asym}(COO), and ν_{sym}(COO) stretching vibrations are observed at (3448, 1727, 1590, and 1396) cm^{-1} for the free ligand. The participation of the carboxylate O atom in the complex formation is evidenced from the shift in the position of these bands to (1691 to 1731) cm^{-1} or the disappearance of the bands between (1550 to 1594) cm^{-1} and (1374 to 1395) cm^{-1} for norfloxacin−metal complexes. For comparison the carbonyl-O; ν(C═O), stretching vibration is found in the free ligand at 1716 cm^{-1}. This band is shifted to lower wavenumbers [(1615 to 1691) cm^{-1}] in the complexes indicating the participation of the carbonyl-O in coordination. There are three new bands found in the spectra of the complexes in the regions (529 to 420) cm^{-1}, which are assigned to ν(M−O) stretching vibrations of carboxylate-O and carbonyl-O.

The IR spectra of all complexes except for the $[Cr_2(L)_2$-$(CO_3)_2(H_2O)_4]$ and $[Mn(L)_2(H_2O)_2]$ complexes show a sharp broad absorption near 3400 cm^{-1} and a group of bands with different intensity in the range (2800 to 2700) cm^{-1} and (2500 to 2400) cm^{-1}. These bands are assigned to the vibration of the quaternized nitrogen of the piperazinyl group which indicates that the zwitterionic form of norfloxacin (Figure 1) is involved in the coordination to the metal ions investigated.[20−22]

The bands associated with the bridged carbonato ligand in the $[Cr_2(L)_2(CO_3)_2(H_2O)_4]$ complex are assigned as follows. The symmetric $\nu_s(CO_2)/\nu_1$ is observed at 1453 cm^{-1}, while the antisymmetric $\nu_{as}(CO_2)/\nu_4$ is observed at 1382 cm^{-1} as a strong band. The ν(C−O)/ν_2 vibration in the Cr(III) complex appears as one band of strong intensity at 1030 cm^{-1}. The bending motion, $\delta(CO_2)$, in this complex is assigned at (825 and 784) cm^{-1} with strong and medium intensities, respectively. The assignments of these bands agree quite well with those known for related bridged carbonate complexes.[24]

The $[Cr_2(HL)_2(SO_4)_2(H_2O)_4]SO_4$ and $[Ni(HL)_2(SO_4)]$ complexes possess C_{2v} symmetry where the sulfato ligand acts as a bridging ligand between the two chromium metal ions. Such structures may be stabilized by solid−solid interactions of different molecules. It is well-known that the free sulfate ion belongs to the highly symmetrical point group T_d. If the ion is coordinated to a metal, the symmetry is lowered, and splitting

Table 3. Thermal Data of Norfloxacin and Its Ti(IV), Cr(III), Mn(II), and Ni(II) Complexes

				TGA weight loss (%)		
complexes	steps	temp. range (°C)	DTA peak (°C)	calc.	found	assignments
$[Ti(HL)(Cl)_4]$	1st	30−340	301	42.81	42.14	$CO + HF + CH_2CH_2 + 2Cl_2$
	2nd	340−600	556	43.98	43.76	$C_{14}H_{14}N_3$
	residual					TiO_2
$[Cr_2(L)_2(CO_3)_2(H_2O)_4]$	1st	30−200	116	7.72	7.50	$4H_2O$
	2nd	200−600	337	75.97	76.89	$2\,L + 2CO_3$
	residual					Cr_2O_3
$[Cr(HL)_2(Cl)_2]Cl\cdot 3H_2O$	1st	30−313	160	18.86	20.85	$3/2Cl_2 + 3H_2O$
	2nd	313−394	351	19.97	20.85	2 piperazine ring
	3rd	394−600	404, 449	43.31	42.14	remain 2L moieties
	residual					Cr_2O_3
$[Cr(HL)_2(AcO)_2]AcO\cdot 2H_2O$	1st	30−217	77, 185	10.51	11.20	$AcO + 2H_2O$
	2nd	217−600	351	72.67	71.98	2AcO + 2HL moieties
	residual					Cr_2O_3
$[Cr_2(HL)_2(SO_4)_2(H_2O)_4]SO_4$	1st	30−400	390	35.49	35.39	$HL + 4H_2O$
	2nd	400−600	544	28.96	28.59	HL
	residual					$Cr_2(SO_4)_3$
$[Mn(L)_2(H_2O)_2]$	1st	30−290	80, 103, 217	16.63	16.74	$2H_2O$ + piperazine ring
	2nd	290−398	342	20.75	20.02	$2F + 2CH_2CH_2$ + piperazine
	3rd	398−600	474, 572	47.00	47.03	$C_{20}H_{10}N_2O_4$ moiety
	residual					MnO_2
$[Mn(HL)_2(Cl)_2]$	1st	30−600	306	88.63	88.57	$HL + Cl_2 + C_{16}H_{18}N_3FO$
	residual					MnO_2
$[Mn(HL)_2(AcO)_2]$	1st	30−600	315	89.28	87.93	$2AcO + HL + C_{16}H_{18}N_3FO$
	residual					MnO_2
$[Ni(HL)_2(Cl)_2]$	1st	30−600	297	90.27	88.80	$2HL + Cl_2$
	residual					NiO
$[Ni(HL)_2(SO_4)]$	1st	30−600	327	80.50	80.41	2HL
	residual					$NiSO_4$
$[Ni(HL)_2(AcO)_2]$	1st	30−600	410	90.84	90.26	2HL + 2AcO
	residual					NiO

of the degenerate modes occurs together with the appearance of new bands in the IR spectrum corresponding to Raman-active bands in the free ion. Accordingly, bidentate chelating and bridging sulfato groups belong to the lower symmetry C_{2v}. However, the vibrations of the bidentate sulfate group in these complexes can be assigned for the various SO_4^{2-} modes.[25] Two bands with strong intensities occur in the region above 1000 cm^{-1} at [(1184, 1190) cm^{-1}], [(1107, 1111) cm^{-1}], 1035 cm^{-1}, and [(968, 973) cm^{-1}] assigned to the different symmetic and antisymmetric bond vibrations, $\nu(SO_4)^{2-}$, while the bending motion of $\delta(SO_4)^{2-}$ is assigned to the band at 618 cm^{-1}.

Therefore, from the IR spectra, it is concluded that norfloxacin behaves as a neutral bidentate ligand for all complexes except for both the $[Cr_2(L)_2(CO_3)_2(H_2O)_4]$ and the $[Mn(L)_2(H_2O)_2]$ complexes and binds to the metal ions through protonated carboxylate O and carbonyl groups.

Electronic Absorption Spectra and Magnetic Susceptibility. The formation of the Ti(IV), Cr(III), Mn(II), and Ni(II) complexes was also confirmed by UV−vis spectra. The electronic absorption spectra of the ligand and their complexes in DMSO were obtained in the (200 to 600) nm range. The free norfloxacin has two distinct absorption bands; the first one at 285 nm may be attributed to $\pi\rightarrow\pi^*$ transition of the heterocyclic moiety and phenyl group. The second band observed at 335 nm is attributed to the $n\rightarrow\pi^*$ electronic transition. In the spectra of the norfloxacin complexes, the two bands are hypochromically affected, suggesting that the ligand coordinates to metal ions via carboxylic and ketone groups, which is in accordance with the results of the FTIR spectra.

The magnetic moments of the Cr(III) and Mn(II) complexes lie in the range of [(3.75 to 3.90) BM)] and [(5.88 to 5.96) BM], respectively. The solid reflectance spectra of the Cr(III) complexes exhibit absorption bands in the range (13262 to 19417) cm^{-1}, (24937 to 27397) cm^{-1}, and (37037 to 38022) cm^{-1} due to the $^4A_{2g}(F) \rightarrow {}^4T_{2g}(F)$, $^4A_{2g}(F) \rightarrow {}^4T_{1g}(F)$, and $^4A_{2g}(F) \rightarrow {}^4T_{1g}(P)$ spin allowed $d-d$ transitions, respectively. These bands suggest an octahedral geometry for the Cr(III) complexes (Figure 2).[26]

The electronic spectra of the Mn(II) complexes show absorption bands in the range (16949 to 19531) cm^{-1}, (22222 to 24272) cm^{-1}, and (26315 to 27777) cm^{-1}. These absorption bands are assigned to the $^6A_{1g} \rightarrow {}^4T_{1g}$ (^4G), $^6A_{1g} \rightarrow {}^4T_{2g}$ (^4G), and $^6A_{1g} \rightarrow {}^4E_g$, $^4A_{1g}$ (4G) transitions, respectively. These bands suggest that the Mn(II) complexes possess an octahedral geometry (Figure 3).[26]

The magnetic moment values for the 1:2 nickel(II) complexes are between (3.50 and 3.85) BM which is in the normal range observed for octahedral Ni(II) complexes [μ_{eff} = (2.80 to 4.00) BM].[26] The solid reflectance spectra have two bands at (15552 to 16260) cm $^{-1}$ and (21978 to 21739) cm^{-1} which were assigned to the transitions of $^3A_{2g} \rightarrow {}^3T_{1g}$ (F) and $^3A_{2g} \rightarrow {}^3T_{1g}$ (P), respectively. So, the formed complexes have an octahedral geometry around the Ni(II) ion (Figure 4).

The titanium(IV) complexes reported in the literature[27,28] are all diamagnetic, and most of them are octahedral. Hence it may be reasonably assumed that the norfloxacin/titanium(IV) complex is six-coordinated and octachedral (Figure 5). These results are consistent with the stoichiometry proposed on the basis of the analytical data and also the magnetic moment at 1.71 μ_B.

Thermal Analysis and Thermodynamic Parameters. Herein the thermal studies of the norfloxacin complexes are investigated; the heating rates were controlled at 10 °C·min^{-1} under a static nitrogen atmosphere, and the weight loss was measured from room temperature until 600 °C. The data are listed in Table 3 and shown in Figure 6. The weight losses for each complex were calculated within the corresponding temperature ranges. The different thermodynamic parameters are listed in Table 4.

The TG curve of the titanium(IV)−norfloxacin complex shows two significant steps in the decomposition. In the first step, the loss of $CO + HF + CH_2CH_2 + 2Cl_2$ molecules occurs in the temperature range (30 to 340) °C with a mass loss of

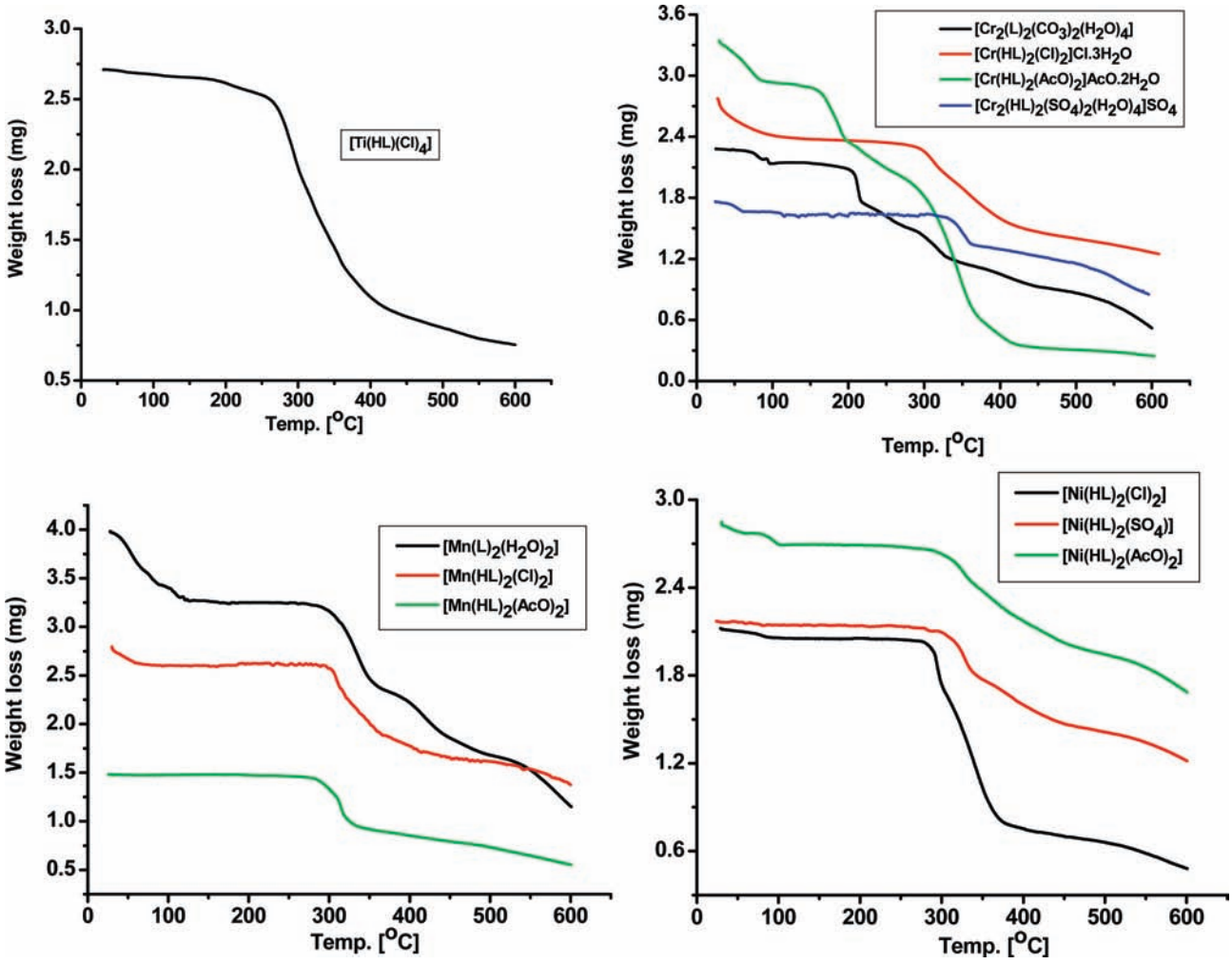

Figure 6. TGA/DTA curves of: $[Ti(HL)(Cl)_4]$, $[Cr_2(L)_2(CO_3)_2(H_2O)_4]$, $[Cr(HL)_2(Cl)_2]Cl\cdot 3H_2O$, $[Cr(HL)_2(AcO)_2]AcO\cdot 2H_2O$, $[Cr_2(HL)_2(SO_4)_2(H_2O)_4]SO_4$, $[Mn(L)_2(H_2O)_2]$, $[Mn(HL)_2(Cl)_2]$, $[Mn(HL)_2(AcO)_2]$, $[Ni(HL)_2(Cl)_2]$, $[Ni(HL)_2(SO_4)]$, and $[Ni(HL)_2(AcO)_2]$ complexes.

Table 4. Thermodynamic Parameters Using the Coats−Redfern (CR) and Horowitz−Metzger (HM) Operated for Norfloxacin and Its Ti(IV), Cr(III), Mn(II), and Ni(II) Complexes[a]

		average of parameters of (CR + HM)					
		E	A	ΔS	ΔH	ΔG	
compound	stage	kJ·mol^{-1}	s^{-1}	J·mol^{-1}·K^{-1}	kJ·mol^{-1}	kJ·mol^{-1}	r
A	1	35.54	$2.24\cdot 10^5$	−129.2	37.48	45.23	0.9854
B	1	70.66	$8.32\cdot 10^{14}$	−130	65.44	114.2	0.9876
C	1	55.43	$1.54\cdot 10^8$	−95.32	53.21	112.21	0.9765
D	1	61.41	$2.21\cdot 10^8$	−91.53	55.87	121.32	0.9543
E	1	94.43	$6.22\cdot 10^{14}$	−49.42	93.24	90.54	0.9987
F	1	208	$2.17\cdot 10^{19}$	−51.21	93.44	88.94	0.9543
G	1	101.50	$0.97\cdot 10^7$	−142.6	81.65	177.20	0.9975
H	1	115	$3.21\cdot 10^{15}$	−84.22	114.20	110.4	0.9765
I	1	60.42	$1.41\cdot 10^5$	−151.24	58.34	96.22	0.9654
J	1	50.11	$9.22\cdot 10^7$	−97.44	51.22	92.46	0.9965
K	1	20.66	$3.24\cdot 10^9$	−65.54	16.42	42.62	0.9766

[a] A: $[Ti(HL)(Cl)_4]$, B: $[Cr_2(L)_2(CO_3)_2(H_2O)_4]$, C: $[Cr(HL)_2(Cl)_2]Cl\cdot 3H_2O$, D: $[Cr(HL)_2(AcO)_2]AcO\cdot 2H_2O$, E: $[Cr_2(HL)_2(SO_4)_2(H_2O)_4]SO_4$, F: $[Mn(L)_2(H_2O)_2]$, G: $[Mn(HL)_2(Cl)_2]$, H: $[Mn(HL)_2(AcO)_2]$, I: $[Ni(HL)_2(Cl)_2]$, J: $[Ni(HL)_2(SO_4)]$, and K: $[Ni(HL)_2(AcO)_2]$ complexes.

42.14 % found, (calcd 42.81 %). The decomposition temperature of the second stage lies in the range (340 to 600) °C which corresponds to the loss of the remaining ligand moiety with a mass loss 43.76 % (43.98 %, calcd).

The thermogravimetric curve of the $[Cr_2(L)_2(CO_3)_2(H_2O)_4]$ chelate shows two decomposition steps within the temperature range (30 to 600) °C. The first step of decomposition is within the temperature range (30 to 200) °C and corresponds to the loss of four water molecules with a mass loss of 7.50 % (calcd 7.72 %). The subsequent step [(200 to 600) °C] corresponds to the removal of the organic part of the two ligands and $2CO_3$, leaving metal oxide as the residue. The overall weight loss amounts to 84.39 % (calcd 83.69 %). Meanwhile, the TG curve of the $[Cr(HL)_2(Cl)_2]Cl\cdot 3H_2O$ chelate shows three stages of decomposition within the temperature range of (30 to 600) °C. The first stage at (30 to 313) °C corresponds to the loss of $3/2Cl_2 + 3H_2O$ molecules with a mass loss of 20.85 % (calcd 18.86 %). The second and third steps involve the loss of two piperazine

rings and the remaining 2L moieties, respectively, with a mass loss of 62.99 % (calcd 63.28 %). The $[Cr(HL)_2(AcO)_2]$-$AcO \cdot 2H_2O$ complex was thermally decomposed in two decomposition steps within the temperature range of (30 to 600) °C. The estimated mass loss of 83.18 % (calcd = 83.18 %) may be attributed to the liberation of the $3AcO + 2H_2O$ and 2HL molecules leaving Cr_2O_3 as the residue. In addition, the $[Cr_2(HL)_2(SO_4)_2(H_2O)_4]SO_4$ complex decomposes in two successive steps within the temperature range (30 to 600) °C with a mass loss of 64.45 % (calcd 63.98 %) leaving $Cr_2(SO_4)_3$ as residue.

On the other hand, the $[Mn(L)_2(H_2O)_2]$ and $[Mn(L)_2Cl_2]$ chelates exhibit three and one decomposition steps, respectively. In the $[Mn(L)_2(H_2O)_2]$ complex, the first step in the temperature range (30 to 290) °C (mass loss = 16.74 % (calcd 16.63 %)) accounts for the loss of $2H_2O$ + piperazine ring. The second step occurs at $T_{G_{max}} = 342$ °C which ranged within (290 to 398) °C with a mass loss = 20.02 % (calcd 20.75 %) and is assigned to $2F + 2CH_2CH_2$ + piperazine moieties. The final decomposition step occurs at (398 to 600) °C accompanied by a mass loss = 47.03 % (calcd 47.00 %) with the loss of a $C_{20}H_{10}N_2O_4$ moiety. As shown in Table 3, the mass loss of the $[Mn(L)_2Cl_2]$ complex is 88.57 % (calcd 88.63 %) in one step which is assigned to $HL + Cl_2 + C_{16}H_{18}N_3FO$. The $[Mn(HL)_2(AcO)_2]$ complex was thermally decomposed in one decomposition step within the temperature range of (30 to 600) °C. The estimated mass loss of 87.93 % (calcd = 89.28 %) is attributed to the liberation of the 2AcO and 2HL molecules leaving MnO_2 as the residue.

The TG curves of the nickel(II) complexes $[Ni(HL)_2(Cl)_2]$, $[Ni(HL)_2(SO_4)]$, and $[Ni(HL)_2(AcO)_2]$ all have only one decomposition step as shown in Table 3. The decomposition step occurs within the temperature range (30 to 600) °C corresponding to the loss of $2HL + Cl_2$, 2HL, and $2HL + 2AcO$, respectively, with a mass loss of (88.80, 80.41, and 90.26) % (calcd 90.27 % for $[Ni(HL)_2Cl_2]$, calcd for 80.50 % for $[Ni(HL)_2(SO_4)]$, and calcd 90.84 % for $[Ni(HL)_2(AcO)_2]$), respectively.

The thermodynamic activation parameters of the decomposition processes of the norfloxacin complexes, namely, activation energy E ($kJ \cdot mol^{-1}$), enthalpy ΔH ($kJ \cdot mol^{-1}$), entropy ΔS ($J \cdot mol^{-1} \cdot K^{-1}$), and Gibbs energy change of the decomposition ΔG ($kJ \cdot mol^{-1}$) were evaluated graphically by employing the Coats−Redfern and Horowitz−Metzger relations.[29,30] The entropy of activation (ΔS^*), enthalpy of activation (ΔH^*), and the free energy change of activation (ΔG^*) were calculated using the following equations:

$$\Delta S^* = 2.303[\log(Ah/kT)]R \quad (1)$$

$$\Delta H^* = E^* - RT \quad (2)$$

$$\Delta G^* = \Delta H^* - T\Delta S^* \quad (3)$$

where A is the Arrhenius constant (s^{-1}); h is the Planck constant; k is the Boltzmann constant; T is the temperature at interval of the decomposition; and R is the gas constant ($J \cdot K^{-1} \cdot mol^{-1}$).

The kinetic thermodynamic parameters of the thermal decomposition data of the norfloxacin complexes are summarized in Table 4. The activation energies of decomposition were found to be in the range (20.66 to 208) $kJ \cdot mol^{-1}$. The high values of the activation energies reflect the thermal stabilities of the complexes.[20−22] The entropy of activation was found to have negative values in all the complexes which indicates that the decomposition reactions proceed with a lower rate than the normal ones.

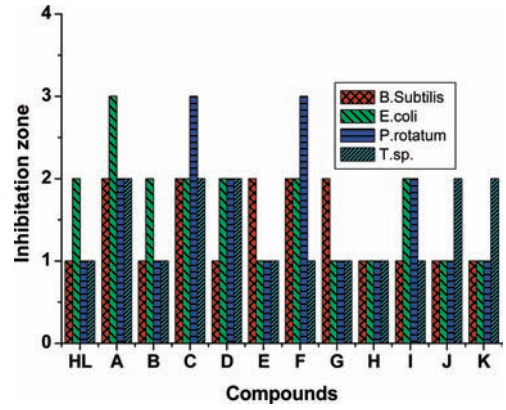

Figure 7. Biological evaluation for norfloxacin and its Ti(IV), Cr(III), Mn(II), and Ni(II) complexes.

Antimicrobial Activity. Antibacterial and antifungal activities of the norfloxacin ligand and its complexes are carried out against the *E. coli* (Gram − ve) and *B. subtilis* (Gram + ve) and antifungal (tricoderma and penicillium) activities. The results of the antimicrobial tests are illustrated graphically in Figure 7. The antimicrobial activity is estimated on the basis of the size of the inhibition zone around the dishes. The norfloxacin complexes are found to have high activity against *E. coli* and *P. rotatum*, whereas the $[Ni(HL)_2(SO_4)]$ and $[Ni(HL)_2(AcO)_2]$ complexes are more active than the other complexes against tricoderma.

Literature Cited

(1) Chu, D. T. W.; Fernandes, P. B. *Advances in Drug Research*; Academic Press: London, 1991; Vol. 21, pp 39−144.
(2) Reynolds, J. E. F. *The Extra Pharmacopeia*, 30th ed.; The Pharmaceutical Press: London, 1993; pp 145−147.
(3) Liang-Cai, Y.; Zi-Long, T.; Pin-Gui, Y.; Sheng-Li, L.; Xia, L. Hydrothermal syntheses, crystal structures and antibacterial activities of two Cu(II) complexes with quinolones. *J. Coord. Chem.* **2008**, *61* (18), 2961–67.
(4) Neu, H. C. Ciprofloxacin-An overview and prospective appraisal. *Am. J. Med.* **1987**, *82*, 395–404.
(5) Xia, Y.; Yang, Z. Y.; Morrisnatschke, S. L.; Lee, K. H. Recent Advances in the Discovery and Development of Quinolones and Analogs as Antitumor Agents. *Curr. Med. Chem.* **1999**, *6*, 179–194.
(6) Valisena, S.; Palumbo, M.; Parolin, C.; Palu, G.; Meloni, G. A. Relevance of ionic effects on norfloxacin uptake by *escherichia coli*. *Biochem. Pharmacol.* **1990**, *40*, 431–6.
(7) Polk, R. E. Drug-drug interactions with ciprofloxacin and other fluoroquinolones. *Am. J. Med.* **1989**, *87* (5A), 76S–81S.
(8) Achari, A.; Neidle, S. Nalidixic acid. *Acta Crystallogr., Sect. B* **1976**, *32*, 600–2.
(9) Huber, C. P.; Sake Gowda, D. S.; Ravindra Acharya, K. Refinement of the structure of nalidixic acid. *Acta Crystallogr., Sect. B* **1980**, *36*, 497–9.
(10) Toffoli, P. P.; Rodier, N.; Ceolin, R.; Blain, Y. Méthanesulfonate de péfloxacinium (péflacine DCI). *Acta Crystallogr., Sect. C* **1987**, *43*, 1745–8.
(11) Parvez, M.; Arayne, M. S.; Sultana, N.; Siddiqi, A. Z. Pefloxacinium methanesulfonate 0.10-hydrate. *Acta Crystallogr., Sect. C* **2000**, *56*, 910–2.
(12) Rosales, M. J.; Toscano, R. A.; Barba-Behrens, N.; Garcia, J. Structure of the antimicrobial agent cinoxacin. *Acta Crystallogr., Sect. C* **1985**, *41*, 1825–6.
(13) Golic, L.; Sustar, B.; Barbo, M. Joint Slovenian-Croatian Crystallographic Meeting, Otocec, Book of Abstracts, 1992; p 25.
(14) Florence, A. J.; Kennedy, A. R.; Shankland, N.; Wright, E.; Al-Rubayi, A. Norfloxacin dehydrate. *Acta Crystallogr., Sect. C* **2000**, *56*, 1372–3.
(15) Turel, I.; Bukovec, P.; Quirós, M. Crystal structure of ciprofloxacin hexahydrate and its characterization. *Int. J. Pharm.* **1997**, *152*, 59–65.
(16) Prasanna, M. D.; Guru Row, T. N. Hydrogen bonded networks in hydrophilic channels: crystal structure of hydrated Ciprofloxacin Lactate and comparison with structurally similar compounds. *J. Mol. Struct.* **2001**, *559*, 255–61.

(17) Wallis, S. C.; Gahan, L. R.; Charles, B. G.; Hambley, T. W. ^{13}C NMR and Single-Crystal X-Ray Structural Investigation of the Fluoroquinolone Antimicrobial Drug Norfloxacin 2DCl·D_2O. *Aust. J. Chem.* **1994**, *47*, 799–806.

(18) Turel, I.; Gruber, K.; Leban, I.; Bukovec, N. Synthesis, crystal structure, and characterization of three novel compounds of the quinolone family member (norfloxacin). *J. Inorg. Biochem.* **1996**, *61*, 197–212.

(19) Chen, Z. F.; Xiong, R. G.; Zuo, J. L.; Guo, Z.; You, X. Z.; Fun, H. K. X-Ray crystal structures of Mg^{2+} and Ca^{2+} dimers of the antibacterial drug norfloxacin. *J. Chem. Soc., Dalton Trans.* **2000**, 4013–4.

(20) Sadeek, S. A.; Refat, M. S.; Hashem, H. Complexation and thermogravimetric investigation on tin(II) and tin(IV) with norfloxacin as antibacterial agent. *J. Coord. Chem.* **2006**, *59* (7), 759–75.

(21) Refat, M. S. Synthesis and characterization of norfloxacin-transition metal complexes (group 11, IB): spectroscopic, thermal, kinetic measurements and biological activity. *Spectrochim. Acta, Part A* **2007**, *68* (5), 1393–1405.

(22) Refat, M. S.; Mohamed, G. G.; de Farias, R. F.; Powell, A. K.; El-Garib, M. S.; El-Korashy, S. A.; Hussien, M. A. Spectroscopic, thermal and kinetic studies of coordination compounds of Zn(II), Cd(II) and Hg(II) with norfloxacin. *J. Therm. Anal. Calorim.* **2010**, in press.

(23) Gupta, R.; Saxena, R. K.; Chaturvedi, P.; Virdi, J. S. Chitinase production by *Streptomyces viridificans*: its potential on fungal cell wall lysis. *J. Appl. Bacteriol.* **1995**, *78*, 378–83.

(24) Beattie, I. R.; Gilson, T. R.; Ozin, G. A. Single-crystal Raman spectroscopy of square-planar and tetrahedral $CuCl_4^{2-}$ ions, of the $ZnCl_4^{2-}$ Ion, and of $CuCl_2$, $2H_2O$. *J. Chem. Soc. A* **1969**, 534–41.

(25) Nakamoto, K. *Infrared and Raman Spectra of Inorganic and Coordination Compounds*; Wiley: New York, 1978.

(26) Cotton, F. A.; Wilkinson, G.; Murillo, C. A.; Bochmann, M. *Advanced Inorganic Chemistry*, 6th ed.; Wiley: New York, 1999.

(27) Entley, W. R.; Treadway, C. R.; Wilson, S. R.; Girolami, G. S. The Hexacyanotitanate Ion: Synthesis and Crystal Structure of $[NEt_4]_3[Ti^{III}(CN)_6]$·4MeCN. *J. Am. Chem. Soc.* **1997**, *119*, 6251–8.

(28) Seetharamappa, J.; Keshavan, B. Synthesis, Structural and Thermal Studies of Titanium(IV) Complexes of *N*-Alkyl Phenothiazines. *Turk. J. Chem.* **1999**, *23*, 429–34.

(29) Coats, A. W.; Redfern, J. P. Kinetic parameters from thermogravimetric data. *Nature* **1964**, *201*, 68–9.

(30) Horowitz, H. W.; Metzger, G. A new analysis of thermogravimetric traces. *Anal. Chem.* **1963**, *35*, 1464–8.

Received for review January 20, 2010. Accepted May 29, 2010.

JE100064H